PHYSICAL REVIEW A VOLUME 46, NUMBER 7 1 OCTOBER 1992

Hexagonal patterns in optical bistability

W. J. Firth,* A. J. Scroggie, and G. S. McDonald†
Department of Physics and Applied Physics, John Anderson Building, 107 Rottenrow, Glasgow, G4 0NG, United Kingdom

L. A. Lugiato
Dipartimento di Fisica, Universita di Milano, Via Celoria 16, Milano, Italy
(Received 8 June 1992)

The mean-field model of optical bistability in a ring cavity is extended to include diffraction in two transverse dimensions. Nonlinear analysis in the neighborhood of the instability of the homogeneous solution indicates the formation of stable hexagonal patterns, and this is confirmed by numerical simulation, with reasonable quantitative agreement. Simulations with higher excitation show defect structures.

PACS number(s): 42.65.Jx, 42.65.Pc

I. INTRODUCTION

Transverse effects in nonlinear ring-cavity systems have been extensively analyzed from 1982 by Moloney and others [1,2]. Analytical investigations with diffractive coupling in one transverse dimension have demonstrated that static and dynamic transverse structures occur in this system. Extension of the mean-field model developed from optical bistability to include diffraction [3] independently demonstrated qualitatively similar features, again in one transverse dimension.

Investigations in two transverse dimensions have been largely confined to numerical studies by Moloney *et al.* [1], showing for Gaussian beam illumination ring structures which develop through azimuthal instability to a pattern of spots which typically execute a slow chaotic dance.

Here we have undertaken numerical investigations of the equation describing the mean-field model of optical bistability [3], showing that roll patterns are unstable to hexagon formation. Thus one-dimensional simplifications of pattern-forming systems of this kind are qualitatively as well as quantitatively inadequate to describe experiments, except where one transverse dimension is suppressed, for example, by a wave-guide structure. The numerical investigations indicate that hexagons are stable over a range below the instability threshold of the plane-wave solution. Defect structures in the patterns are also observed.

II. HEXAGON FORMATION AND SIMPLIFIED MODELS

In cavityless counterpropagating beam configurations hexagonal structures have recently been experimentally observed [4] and subjected to intensive numerical and analytic study [5,6]. Hexagons typically arise from a quadratic nonlinear coupling in a system with an unstable transverse wave vector. In optical media with third-order nonlinearity, a quadratic type of nonlinearity arises when an external driving field provides a phase reference and lowers the symmetry. Physically, forward four-wave mixing has these characteristics [4]. All these considerations suggest that not only the bidirectional Fabry-Pérot cavity geometry, but also the unidirectional ring-cavity geometry ought to be suitable for hexagonal pattern formation, and we present here a combination of analytical and numerical evidence that this is indeed the case.

We start from the two-dimensional extension of the model of [3], which describes a Kerr medium in a cavity with flat mirrors driven by a coherent plane-wave field:

$$\frac{\partial E}{\partial \tau} = -E + E_I + i\eta(|E|^2 - \theta)E + ia\nabla_\perp^2 E \tag{1}$$

wherein the input field E_I breaks the phase-rotational symmetry for E. The parameter η equals $+1$ (-1) for self-focusing (self-defocusing) Kerr media. The symbol θ denotes the detuning parameter. The time τ is defined as t/t_{ph}, where t_{ph} is the mean lifetime of photons in the cavity which is given by cT/L for a unidirectional ring cavity and by $cT/2L$ for a Fabry-Pérot cavity (where L is the cavity length and T is the transmission coefficient of the cavity mirrors). The transverse Laplacian is defined as $\nabla_\perp^2 = \partial^2/\partial x'^2 + \partial^2/\partial y'^2$, $x' = x/b$, $y' = y/b$ where b is an arbitrary length, introduced in order to make the parameter a dimensionless; a is defined as $c\lambda t_{ph}/4\pi b^2$ (λ is the wavelength). The relevance of (1) as a simplification of full counterpropagation equations with mirror boundary conditions is underlined by an alternative derivation, using a pole analysis, to describe the field within a Fabry-Pérot resonator [7].

Model (1) is transformed into an equation for the deviation A (not necessarily small) of the circulating field from its plane-wave steady-state value E_s:

$$\frac{\partial A}{\partial t} = -[1 + i\eta(\theta - |E_s|^2)]A + i\eta|E_s|^2(A + A^* + A^2 + 2|A|^2 + A|A|^2) + ia\nabla_\perp^2 A \tag{2}$$

where $E = E_s(1 + A)$.

The quadratically nonlinear terms in (2) give the coupling expected to lead to hexagons, while these and the complex conjugate terms betray the phase symmetry breaking of (1) and (2) as compared to, for example, the laser Ginzburg-Landau equation [8].

Equation (2) can be seen as a generalization and reinterpretation of an equation proposed by Courtois and Grynberg [9] as a simplified model for counterpropagating beams in a cavityless Kerr medium [3,4]. If their equation is generalized to the case of a complex parameter $\gamma=\gamma_R+i\gamma_I$, it reads

$$\frac{\partial A}{\partial t'}=-(\gamma_R+i\gamma_I)A+\frac{i}{\theta_0^2}\nabla_\perp^2 A +i\kappa'(A+A^*+A^2+2|A|^2+A|A|^2)\,, \tag{3}$$

where $t'=ct/L$, L is the length of the Kerr medium, κ' is the coupling parameter, and $\theta_0^2=4\pi b^2/\lambda L$. The parameter γ_R is of order unity and γ_I has been introduced to establish the connection with the model in [3].

By defining the rescaled time $\tau=\gamma_R t'$ and the new parameters $\kappa=\eta\kappa'/\gamma_R$ and $\delta=\gamma_I/\gamma_R$, Eq. (3) becomes

$$\frac{\partial A}{\partial \tau}=-(1+i\delta)A+ia\nabla_\perp^2 A +i\eta\kappa(A+A^*+A^2+2|A|^2+A|A|^2)\,. \tag{4}$$

There is then a formal correspondence between Eqs. (2) and (4) if we take $\delta=\eta(\theta-|E_s|^2)$ and $\kappa=|E_s|^2$. We require that $\gamma_R\theta_0^2 a=1$ in order to identify the scalings of the diffraction parameters in (2) and (3). By appropriate choice of transverse scale, a can always be set to unity, and we choose $a=1$ in the numerical simulation described below.

III. LINEAR AND NONLINEAR ANALYSIS

In this section we give a preliminary analysis of (4), along the lines of that given by Courtois and Grynberg [9], primarily to enable comparison with our numerical results. A more complete analysis, considering more general cases than pure hexagonal patterns, will be published elsewhere.

Assuming that any instability has a dependence on the transverse coordinates described by the function $\vartheta(x,y)$ where

$$\nabla_\perp^2\vartheta=-K^2\vartheta \tag{5}$$

and carrying out a linear stability analysis of the $A=0$ solution of (4), the following expression for the threshold curves is obtained [3]:

$$\kappa=\frac{1+(\delta+aK^2)^2}{2\eta(\delta+aK^2)}\,. \tag{6}$$

For a given value of δ each curve has a minimum in the (aK^2,κ) plane at the point (aK_c^2,κ_c) given by

$$\kappa_c=1=\eta(\delta+aK_c^2)\,. \tag{7}$$

$2\pi/K_c$ is then the magnitude of the most unstable wavelength (in units of b) and κ_c is the critical value of the control parameter κ at which a bifurcation is expected to occur.

When $\kappa>\kappa_c$ a continuous band of wave vectors becomes unstable. In the self-focusing case this phenomenon can arise both when the steady-state curve of $|E_s|^2$ as a function of $|E_I|^2$ is single-valued and when it is S shaped (bistability), whereas for $\eta=-1$ the system can be unstable to finite-wave-vector instabilities only in the bistable regime. Since in the case $\eta=-1$ the instability region lies mostly within the unstable middle branch of the bistable curve and partly in the stable lower branch, the only expected effect of an inhomogeneous perturbation in the unstable region is to switch the cavity field to the stable upper branch [10]. Stationary transverse patterns are therefore expected to be unobservable for defocusing media.

Introducing $\mathbf{V}=[R,I]^T$ where R and I are the real and imaginary parts of A, respectively [9], the nature of any bifurcation at the critical point can be determined by a perturbation expansion of $\mathbf{V}$ and κ in powers of a small parameter ϵ around the bifurcation point [11]:

$$\mathbf{V}=\epsilon\mathbf{V}^{(1)}+\epsilon^2\mathbf{V}^{(2)}+\epsilon^3\mathbf{V}^{(3)}+\cdots\,, \tag{8}$$

$$\kappa=\kappa_c+\epsilon\kappa^{(1)}+\epsilon^2\kappa^{(2)}+\epsilon^3\kappa^{(3)}+\cdots\,. \tag{9}$$

Solutions of the form $\mathbf{V}=\mathbf{v}\vartheta(x,y)$ are sought where $\vartheta(x,y)$ is the hexagon mode having a transverse wave vector of magnitude K_c. Substituting (8) and (9) into (4) and separating the different orders in ϵ gives, at each order ϵ^i, a matrix equation of the form

$$L\mathbf{V}^{(i)}=\begin{pmatrix}-1 & \delta-a\nabla_\perp^2\\ 2\eta-\delta+a\nabla_\perp^2 & -1\end{pmatrix}\mathbf{V}^{(i)}=\mathbf{S}^{(i)}\,, \tag{10}$$

where, in general, $\mathbf{V}^{(i)}$ and $\mathbf{S}^{(i)}$ are Fourier analyzed into their separate spatial frequency components, $\mathbf{V}_{K^2}^{(i)}$ and $\mathbf{S}_{K^2}^{(i)}$, so that each $\mathbf{V}^{(i)}$ is a sum of eigenfunctions of the transverse Laplacian.

It is found that $\mathbf{S}^{(1)}=0$ so that the matrix L must be singular for $K^2=K_c^2$. This means that for $i>1$ L is singular for all resonant terms (those with $K^2=K_c^2$) and a solvability condition (Fredholm's Alternative) must be applied [9]. This states that for $L\mathbf{V}_{K_c^2}^{(i)}=\mathbf{S}_{K_c^2}^{(i)}$ to have a solution, $\mathbf{S}_{K_c^2}^{(i)}$ must be orthogonal to the kernel of the operator adjoint to L. Imposing this condition allows the determination of $\kappa^{(i-1)}$. For hexagons $\kappa^{(1)}\neq 0$, a result of the fact that ϑ^2 has a spectrum $K=0$, K_c, $\sqrt{3}K_c$, $2K_c$. The bifurcation is therefore predicted to be transcritical [11].

Another approach [9] is to expand the field A over a basis of Fourier modes Φ_n,

$$A=\sum_{n=0}^{\infty}A_n(\tau)\Phi_n\,, \tag{11}$$

and keep only the first two modes. This is justified in that not too far above threshold it is expected that higher harmonics will have negligible amplitudes. Writing A_0 and A_1 as

$$A_0=a_0(\tau)+ia_0'(\tau)\,, \tag{12}$$

$$A_1=a_1(\tau)+ia_1'(\tau) \tag{13}$$

gives a system of four coupled nonlinear ordinary differential equations, whose fixed points represent stationary solutions of (4).

We have determined the amplitudes of the hexagonal patterns predicted by both these methods and compared them with the numerical investigations described below.

IV. NUMERICAL SIMULATION

Simulations have involved integration of both Eq. (1), using a split-step method [12], and Eq. (2), using a finite-difference hopscotch method [13] which involves splitting a square grid into even and odd points and alternating explicit and implicit integration steps on each grid. The grid used is typically 64×64 points for the split-step method and 128×128 for the hopscotch, both with periodic boundary conditions. Since the numerical techniques used by the two codes are of completely different character, each one acts as a good check for the other.

Above the linear threshold a pure "roll"—modulation of the form $\cos(K_c x)$—as the initial condition leads to a stationary roll pattern, but on adding a small amplitude noise component the rolls become unstable and hexagons form instead. Other initial conditions, such as small amplitude noise around the flat solution, generally lead only to hexagonal patterns, as in Fig. 1.

For the case where $\delta=0$ and $\eta=1$, Fig. 2 compares the hexagon amplitude as a function of the control parameter κ predicted by each of the analytical techniques in Sec. III with the results obtained by numerical integration of Eq. (4). The results shown were obtained by starting the simulation about 6% above the linear threshold and, after the stationary hexagonal pattern had been reached, moving up (or down) the stable hexagon branch. In particular it can be seen that the regime of coexistence of the stable hexagon and flat solutions, as given by the modal expansion calculation, is narrower than depicted in [9], extending no more than 3% below the linear threshold. The numerical studies agree quite well with this small extent of coexistence.

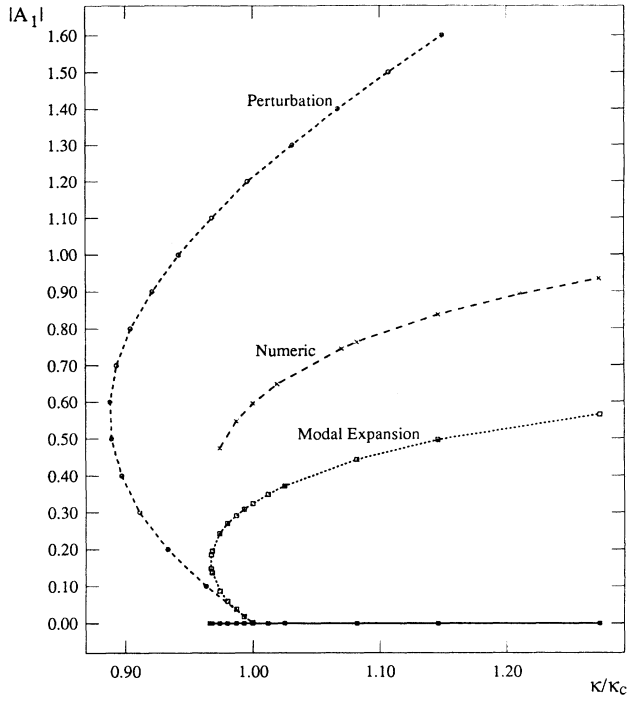

FIG. 2. Comparison of the amplitude of the hexagon pattern, as given by perturbation and modal expansion calculations and by numerical integration, for the case $\delta=0$.

Starting the simulations further above the linear threshold can produce defected patterns as in Fig. 3 (for the case

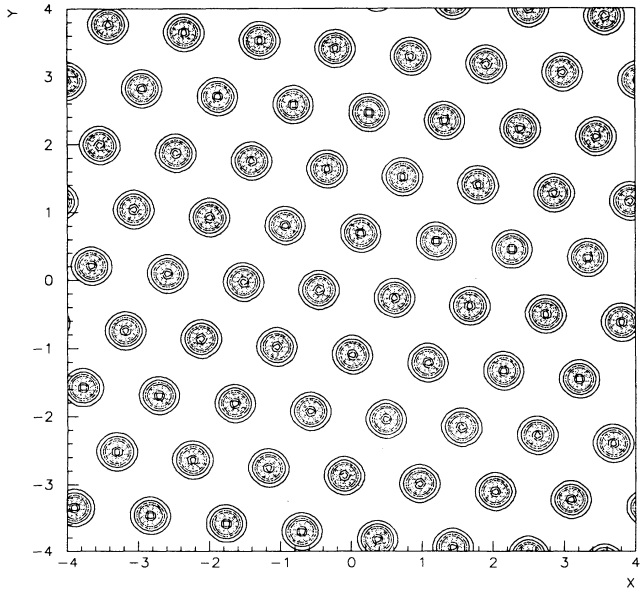

FIG. 1. Contour plot of a stationary hexagon pattern (real part of the field A) in the transverse plane, obtained at 7% above the linear instability threshold. Mean-field, $\eta=1$, $\delta=0$, $a=1$, and plane-wave pumping.

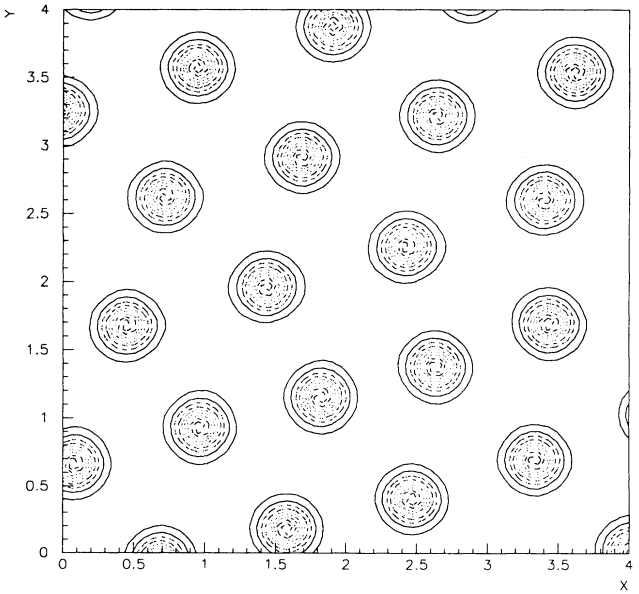

FIG. 3. Penta-hepta defect in the pattern obtained at 27% above threshold, with parameters the same as in Fig. 1. The two spots just to the right of center have, respectively, five and seven neighbors.

of 27% above threshold). Once established, these defects persist throughout the length of the simulation, typically several thousand time steps, but decreasing the parameter κ causes them to anneal to a hexagonal pattern.

V. CONCLUSIONS

The features revealed by the numerical simulations, such as the existence and stability of hexagons below the linear threshold, the instability of rolls, and the existence of defects, are typical of hexagon-forming systems, and some of them are well explained by the nonlinear analysis of (4). Our treatment shows that theory can predict the onset of hexagons also in unidirectional propagation. A key point about these results is that they are obtained in the framework of a model which does not demand supercomputer resources on the one hand, and for which there is considerable experience and expertise in experimental realization, on the other.

ACKNOWLEDGMENTS

This work is supported in part by Science and Engineering Council Grants No. GR/F 76502, No. GR/F 49811, and No. GR/G 12665, in part by a Twinning contract of the European Communities, and in part by the ESPRIT Basic Research Action No. 7118 (TONICS). A.S. acknowledges support from SERC.

---

*FAX number (U.K.): 41 552 2891.

†Present address: Université Libre de Bruxelles, Optique Non-Linéaire Théorique, Campus Plaine C.P.231, B-1050 Bruxelles, Belgium.

[1] J. V. Moloney, H. Adachihara, R. Indik, C. Lizaragga, R. Northcutt, D. W. McLaughlin, and A. C. Newell, J. Opt. Soc. Am. B **7**, 1039 (1990), and references therein.

[2] N. B. Abraham and W. J. Firth, J. Opt. Soc. Am. B **7**, 951 (1990), and references therein.

[3] L. A. Lugiato and R. Lefever, Phys. Rev. Lett. **58**, 2209 (1987).

[4] G. Grynberg, E. LeBihan, P. Verkerk, P. Simoneau, J. J. R. Leite, D. Bloch, S. Le Boiteaux, and M. Ducloy, Opt. Commun. **66**, 321 (1988).

[5] R. Chang, W. J. Firth, R. Indik, J. V. Moloney, and E. M. Wright, Opt. Commun. **88**, 167 (1992).

[6] G. D'Alessandro and W. J. Firth, Phys. Rev. Lett. **66**, 2597 (1991).

[7] M. Haelterman, M. Tolley, and G. Vitrant, J. Appl. Phys. **67**, 2725 (1990); M. Haelterman, G. Vitrant, and R. Reinisch, J. Opt. Soc. Am. B **7**, 1309 (1990); M. Haelterman, Opt. Commun. **75**, 165 (1990).

[8] L. Gil, E. Emilsson, and G.-L. Oppo, Phys. Rev. A **45**, 567 (1992).

[9] J. Y. Courtois and G. Grynberg, Opt. Commun. **87**, 186 (1992).

[10] L. A. Lugiato, Wang Kaige, and N. B. Abraham (unpublished).

[11] P. Manneville, *Dissipative Structures and Weak Turbulence* (Academic, New York, 1990).

[12] R. H. Hardin and F. D. Tappert, SIAM Rev. **15**, 423 (1973).

[13] A. R. Gourlay, J. Inst. Math. Its Appl. **6**, 375 (1970); A. R. Gourlay and G. R. MacGuire, *ibid.* **7**, 216 (1971).